doi: 10.1093/pasj/xxx000

# Stochastic Star Formation in the Milky Way Inferred from the Unity Index of KS law

**Yoshiaki SOFUE**[1]

[1]Institute of Astronomy, The University of Tokyo, Mitaka, Tokyo 186-0015, Japan

*E-mail: sofue@ioa.s.u-tokyo.ac.jp

Received ; Accepted

## Abstract

Using archival CO line data and a catalog of HII regions, we performed a correlation analysis between the brightness temperature of the CO line and number density of HII regions on the longitudinal velocity diagram (LVD) of the Milky Way. The power-law index (exponent) of the Kennicutt-Schmidt (KS) law for molecular gas is determined to be $\alpha = 1.052 \pm 0.207$ and $1.043 \pm 0.119$ for $^{12}$CO line data from the Nobeyama 45-m and Columbia 1.2-m Galactic plane surveys, respectively. This result is consistent with the KS index currently determined for molecular gas not only in the Milky Way, but also in spiral and starburst galaxies. We argue that an index close to 1 is universal in favor of stochastic (spontaneous) star formation, but is inconsistent with cloud collision models that predict a steeper index of $\alpha = 2$. We also showed that the efficiency of star formation in the Galactic Centre is an order of magnitude lower than that in the disc.

**Key words:** Galaxy: evolution — ISM: HII regions — ISM: clouds — ISM: molecules — stars: formation

## 1 Introduction

The trigger of star formation (SF) in the molecular clouds in the Galaxy has been one of the fundamental subjects of the ISM over the decades (Shu et al. 1987; Lada & Lada 2003). There appear two major ideas: one scenario is the stochastic (spontaneous) SF by self-regulation mechanisms in individual molecular clouds due to the gravitational instability and/or sequential compression by expanding shells of HII regions (Elmegreen & Lada 1977; Myers 2009; Hacar et al. 2023; Pineda et al. 2023). Another scenario is the external triggering by collisions of molecular clouds (Habe & Ohta 1992; Hasegawa et al. 1994; Kimura & Tosa 1996; Fukui et al. 2021).

A possible way to clarify the SF mechanisms is to check the power-law index $\alpha$ of the Kennicutt-Schmidt (KS) law (Kennicutt & Evans 2012). The stochastic process predicts $\alpha = 1$, where SFR is proportional to the density of clouds. The collision process requires $\alpha = 2$, where the SFR is proportional to the collision frequency of clouds, and hence to the square of number density of clouds. The current measurements have shown $\alpha \sim 1$ in the Milky Way (Fuchs et al. 2009; Sofue 2017; Sofue & Nakanishi 2017; Elia et al. 2022) and spiral galaxies (Komugi et al. 2006; Kennicutt & Evans 2012), which indicated SFR more linearly proportional to the molecular gas density.

The KS law in the Milky Way has been studied using the face-on maps of the molecular and HI gases and of HII regions (Sofue & Nakanishi 2017; Sofue 2017; Spilker et al. 2021; Bacchini et al. 2019; Elia et al. 2022). Recent studies of the face-on transformation (FOT) from the radial velocity to line-of-sight distance have shown that the derived gas distribution is highly sensitive to the rotation curve (RC) (Marasco et al. 2017; Fujita et al. 2023). So, we revisit the KS-law analysis by adopting the most recent rotation curve of the Galaxy (Sofue 2021). We also propose a new, simple and more direct method to derive the KS-law index using the longitude-velocity diagram (LVD) without employing the FOT (Koda et al. 2016). By applying the new method, we determine the KS law index (exponent) for the molecular gas, and discuss the feasibility of the stochastic and collision models for the star formation.

In the analysis, we use the archival data of $^{12}$CO -line emission from the FUGIN (Four-receiver system Unbiased Galactic plane Imaging survey with the Nobeyama 45-m telescope) (Umemoto et al. 2017), Galactic Centre survey (Tokuyama et al. 2019), and Columbia 1.2-m Galactic plane survey (Dame et al. 2001), combined with the WISE (Wide-field Infrared Survey Explore) HII region catalogue (Anderson et al. 2014).

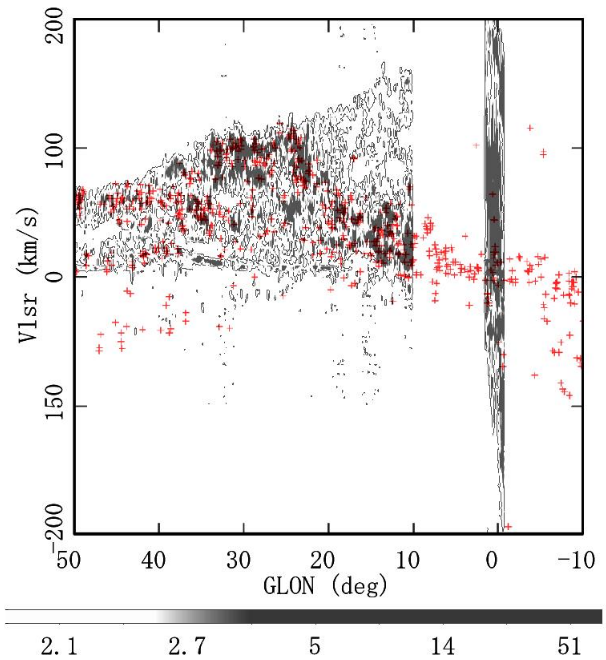


**Fig. 1.** HII regions in the Galactic plane at $|b| \leq 0^\circ.2$ from the WISE catalogue (Anderson et al. 2014) superposed on the LVD of CO-line brightness constructed from the data by the Nobeyama 45-m FUGIN (Umemoto et al. 2017) and GC survey (Tokuyama et al. 2019). The bar indicates $T_{\rm B}$ inK and the contours are drawn at $T_{\rm B} = 0.5$ K.

## 2 Molecular-gas KS law using LVD

We perform correlation analysis on the LVD between the number density of HII regions from the WISE catalogue (Anderson et al. 2014) and the volume density of $H_2$ molecules calculated from the Nobeyama CO-line surveys (Umemoto et al. 2017; Tokuyama et al. 2019) in the inner disc of the Milky Way. Correlation on the LVD is more directly coupled to the data, bypassing the sophisticated face-on transition procedures Koda et al. 2016. Figure 1 plots longitude-velocity positions of HII regions in the Galactic plane superposed on the CO-line LVDs along the Galactic plane ($b = 0^\circ$). As readily known (Hou & Han 2014), HII regions and CO line intensity are tightly correlated in the LVD.

In our study we constrain the region of analysis in the Galactic plane by using only the HII regions in the Galactic plane at $|b| \leq 0^\circ.2$ and CO LVD at $b = 0^\circ$. The region was so chosen in order to avoid the uncertainty during the determination process of the height from the Galactic plane depending on the distance ambiguity. Thus we selected 492 HII regions, about 38% of the 1316 catalogued sources with measurements of LSR velocities in the radio recombination lines (RRL). We then calculate the number density $N$ of HII regions and CO brightness temperature $T_{\rm B}$ averaged in every $(l, v)$ grid with bin size $\delta l \times \delta v = 0^\circ.25 \times 10$

km s$^{-1}$for Nobeyama and $2^\circ \times 5$ km s$^{-1}$for Columbia CO survey data.

Using the thus obtained sets of $N$ and $T_{\rm B}$, we calculate the volume densities $n_i$ of HII regions ($i$ = HII) and $H_2$ molecules ($i = {\rm H_2}$) by

$$n_i = \frac{dN_i}{ds} = \frac{dN_i}{dv}\frac{dv}{ds}, \quad (1)$$

where $v = v_{\rm LSR}$ is the LSR radial velocity and $s$ is the distance from the Sun. Recalling $N_{\rm H_2} = X_{\rm CO}\int T_{\rm B} dv$, we have

$$n_{\rm H_2} = X_{\rm CO} T_{\rm B}(dv/ds), \quad (2)$$

where $X_{\rm CO}$ is the CO-to-$H_2$ conversion factor assumed to be constant at $2 \times 10^{20}$ $H_2$ cm$^{-3}$ [K km s$^{-1}$]$^{-1}$ (Kohno & Sofue 2023). The velocity gradient, $dv/ds$, is calculated by

$$dv/ds = (dV/dR - V/R)k\sqrt{1-k^2}, \quad (3)$$

where $R$ is the galacto-centric radius, $V = V(R)$ is the rotation velocity, $k = R_0 \sin l/R$, and $v$ and $R$ are related by $v = (VR_0/R - V_0)\sin l$. We adopt the most accurate rotation curve of the Milky Way (Sofue 2021; Sofue 2023).

Then, we calculate the following values using the LVD:

$$n^*_{\rm HII} = (dN_{\rm HII}/dv)(dv/ds) \quad (4)$$

and

$$n^*_{\rm H_2} = n_{\rm H_2}/X_{\rm CO} = T_{\rm B}(dv/ds). \quad (5)$$

These quantities are assumed to be proportional to the SFR and the molecular gas density, respectively, averaged in each $\delta v_{\rm LSR} \times \delta l$ bin. The obtained log $n^*_{\rm HII}$ is plotted against log $n^*_{\rm H_2}$ in figure 2. Except for the intensity scaling, the plots are equivalent to the KS plot.

By the least-squares fitting to the plot, adopting the square of standard deviations (bars in the figures) as the statistical weight, we determined the KS-law index (slope in log-log plot). In table 1 we list the results obtained for different longitude ranges. The KS index $\alpha$ for molecular gas is $\alpha = 1.052 \pm 0.207$ for Nobeyama data in the inner disc at $50^\circ \geq l \geq 10^\circ$ (figure 2, panel A), and $1.043 \pm 0.119$ for Columbia data in the entire disc avoiding the central region at $|l| \geq 10^\circ$ (panel B). We find nearly equal value $\alpha = 0.939 \pm 0.116$ inside the 4-kpc molecular ring at $30^\circ \geq |l| \geq 10^\circ$ (panel C) for the Columbia data, and a slightly smaller value $0.892 \pm 0.319$ outside (panel D).

The Nobeyama data in the GC at $|l| \leq 2^\circ$ (panel A, magenta crosses) show significantly lower number density of HII regions despite much higher gas density, showing an order of magnitude lower efficiency of star formation. Accordingly, the Columbia data in the central region at $|l| \leq 10^\circ$ (magenta crosses and line in panel B), which are mixture of the GC and Galactic disc values, indicate lower HII density but with almost the same index of $\alpha = 1.021 \pm 0.110$. The larger number of data points in panel B despite the narrower longitude range is due to steeply increasing velocity range toward the GC.

We emphasize that the present method uses LVDs directly, not intervened by the sophisticated FOT procedure to convert the radial velocity to the distance, which includes the difficulty to discriminate far- and near-side solutions. Therefore, the measured quantities are more reliable compared to those using the current methods in so far as the power-law index of the KS law is concerned. In table 1 we compare the result with the current determination for the Milky Way and spir and starburst galaxies.

The here obtained volumetric index is slightly larger than that those from the current FOT method for the same CO data with $\alpha = 0.7$ to 0.8 (table 1 lines 5 and 6). Also, the surface index for the Milky Way lie at slightly larger values of $\sim 1.15$ (lines 7 to 9). Besides the Milky Way, extensive studies about the KS-law have been obtained in spiral galaxies also indicating mild indices of $\alpha \simeq 0.8 - 1.3$, which are consistent with the present new values. Therefore, we may state that the unity KS-law index is universal. For reference we calculated a simple mean of the listed values except for lines 3 and 4 in table 1 as $\langle\alpha\rangle = 1.056 \pm 0.192$.

On the other hand, a steeper index around $\alpha \sim 1.5$ has been obtained for total gas including HI in spiral galaxies (Kennicutt 1998; Kennicutt & De Los Reyes 2021) and in the Milky Way (Sofue 2017; Sofue 2021). The KS index for the Milky Way using the total surface gas density and SFR from M dwarf stars also yielded $\alpha_{\rm sur} \sim 1.4$ (Fuchs et al. 2009). The difference between the indices of the molecular and total ($H_2$ +HI) gas KS laws would be due to the intervening phase transition from HI to $H_2$ , and vice versa. A more detailed analysis of the correlation between HI and $H_2$ is a subject for a separate paper.

## 3 Discussion

### 3.1 Comparison with KS laws by other methods

The KS law in the Galactic disc defined by the SFR plotted against volume density of molecular gas $\rho$ is given by

$$SFR = A\left(\rho/{\rm H_2cm^{-3}}\right)^\alpha [M_\odot\ {\rm y^{-1}\ kpc^{-3}}]. \quad (6)$$

The 3D molecular gas maps of the Milky Way derived in our earlier works based on the Columbia CO survey and the Hou's HII region catalogue (Hou et al. 2009) made it possible to measure both the volume and surface densities of the HII regions and molecular gas (Sofue 2017; Sofue & Nakanishi 2017). The least-squares fit to the KS plot for molecular gas yielded $\alpha = 0.78 \pm 0.05$ and log $A = -2.6 \pm$

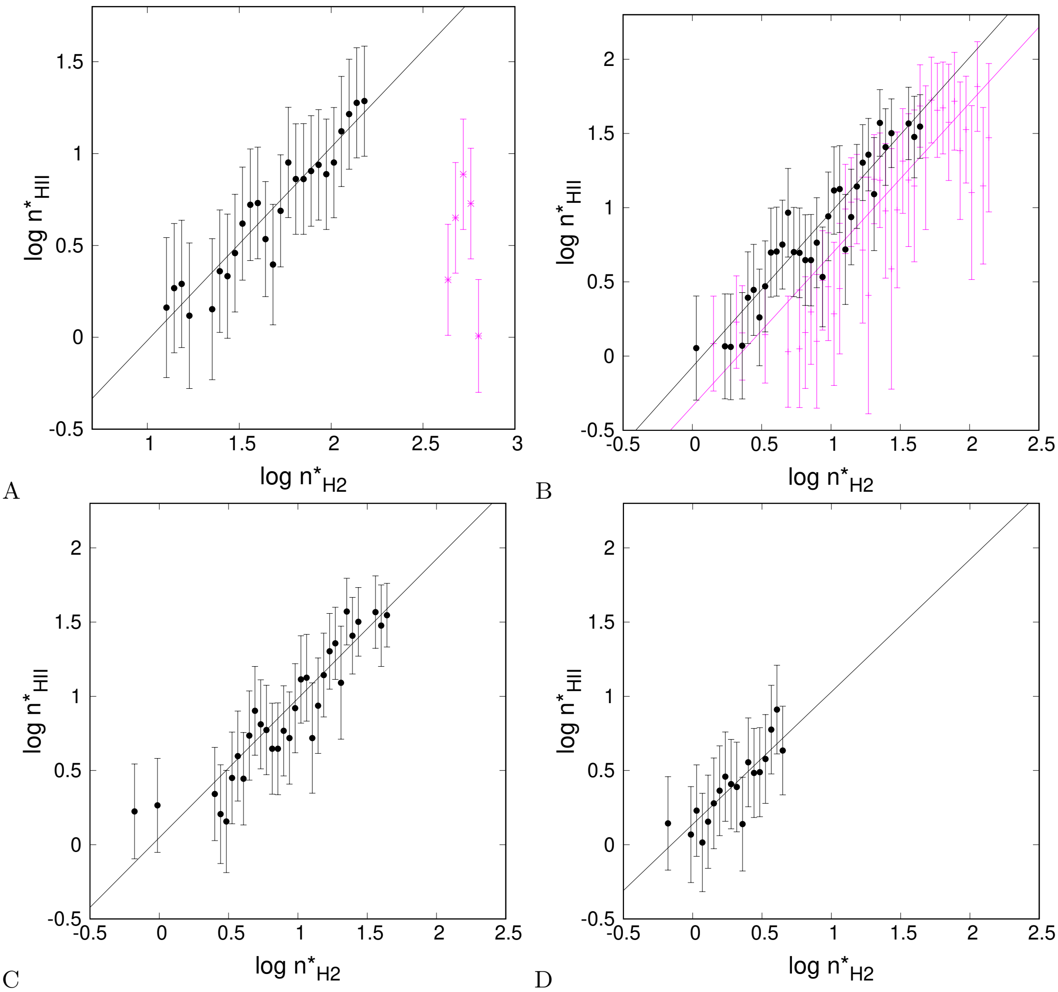


**Fig. 2.** Plots of log $n^*_{\rm H_2}$ using the WISE HII region catalogue against log $n^*_{\rm HII}$ using: [A] Nobeyama 45-m $^{12}$CO at $|l| = 10^\circ - 50^\circ$ and GC $|l| \le 2^\circ$ (magenta). Grid size is $\delta l \times \delta v = 2^\circ \times 5$ km s$^{-1}$. [B] Columbia 1.2 m $^{12}$CO at $|l| = 10^\circ - 180^\circ$ (black) and $|l| \le 10^\circ$ (magenta). Grid size is $0^\circ.25 \times 10 {\rm km\ s^{-1}}$. [C] Columbia $|l| = 10^\circ - 30^\circ$ inside 4 kpc. [D] Columbia $|l| = 30^\circ - 180^\circ$ outside 4 kpc. Bars are standard deviations calculated for the linear values and are converted to logarithmic scaling in the plot. The straight lines are the least-squares fit to the plots.

0.05 for the volume density and $\alpha = 1.12 \pm 0.05$ for surface densities. More recent work for the surface-densities also obtained a value close to unity (Elia et al. 2022).

On the other hand, during the course to derive face-on molecular gas maps of the inner Milky Way (Sofue 2023) based on the most accurate rotation curve (Sofue 2021), it was shown that the kinematical distance is highly sensitive to the adopted rotation curve. This often results in erroneous maps associated with artifact hole and/or over-condensation of gas near and along the tangent-point circle. It was also shown that the maps are strongly disturbed by the non-circular motion such as due to the 3-kpc expanding ring. These problems significantly disturb the KS-law analyses using the face-on maps.This consideration led us to seek for a more direct way to derive the KS law in the Milky Way without employing the face-on maps.

## 3.2 Cloud-collision model with $\alpha = 2$

We here consider the cloud collision process and expected KS law. Let the radius of colliding clouds be $r_{\rm c}$, number density $n_{\rm c}$, and velocity dispersion of the clouds $v_{\rm c}$. Then, we have the mean free path

$$l_{\rm c} = (n_{\rm c} \pi r_{\rm c}^2)^{-1} \tag{7}$$

and collision time

$$t_{\rm c} = l_{\rm c}/v_{\rm c} = (v_{\rm c} n_{\rm c} \pi r_{\rm c}^2)^{-1}. \tag{8}$$

The corresponding SFR is calculated by

$$\mathrm{SFR} = \mathcal{M} n_{\rm c} t_{\rm c}^{-1} = \pi \mathcal{M} n_{\rm c}^2 r_{\rm c}^2 v_{\rm c}, \tag{9}$$

where $\mathcal{M}$ is the specific mass of stars born by one cloud collision. If we assume that the stellar mass fraction born from one colliding cloud is of the order of $\eta = \mathcal{M}/M_{\rm cloud} \sim 0.1$ with the cloud mass $M_{\rm cloud} \sim 10^5 M_\odot$, cloud radius $r_{\rm c} \sim$

**Table 1.** Molecular-gas KS index $\alpha$ (log-log slope) inferred from the correlation of number densities of HII-regions and molecular gas density in the Milky Way and spiral galaxies.

| Object | Index $\alpha$ | Method[†] | Remarks |
|---|---|---|---|
| MW inner disc ($50^\circ \geq l \geq 10^\circ$) | $1.052 \pm 0.207$ | Vol., LVD, Nobe.45m + WISE[‡] | This work (Fig. 2 panel A) |
| MW whole disc ($\lvert l \rvert \geq 10^\circ$) | $1.043 \pm 0.119$ | Vol., LVD, Col.1.2m + WISE | ibid (B) |
| MW inside 4-kpc ring ($30^\circ \geq \lvert l \rvert \geq 10^\circ$) | $0.939 \pm 0.116$ | Vol., LVD, ibid | ibid (C) |
| MW outside 4-kpc ring ($\lvert l \rvert > 30^\circ$) | $0.892 \pm 0.319$ | Vol., LVD, ibid | ibid (D) |
| MW inside $\lvert l \rvert < 10^\circ$ | $1.021 \pm 0.110$ | Vol., LVD, ibid | ibid (B) |
| Milky Way | $0.78 \pm 0.05$ | Vol., 3D, Col. 1.2m + Hou.[†] | (Sofue 2017) |
| Milky Way | 0.73 | Vol. SFR | (Bacchini et al. 2019) |
| Milky Way | $1.12 \pm 0.05$ | Surf. 3D, Col. 1.2m + Hou | (Sofue 2017) |
| Milky Way | $1.14 \pm 0.07$ | Surf., face on | (Elia et al. 2022) |
| MW Solar vici. 2 kpc | $1.19 \pm 0.09$ | Surf., local clouds & HII | Fit to fig. 18 of Spilker et al. 2021 |
| Galaxies: NGC/DDO | 1.081 | Volume | (Kennicutt 1998) |
| NGC/starburst | $1.4 \pm 0.15$ | Surf. | (Kennicutt & De Los Reyes 2021) |
| NGC/DDO | 0.925 | Surf. | (Du et al. 2023) |
| NGC high mol. den. | $1.33 \pm 0.08$ | Surf. | (Komugi et al. 2006) |
| UGC | $0.99 \pm 0.08$ | Surf. | (Komugi et al. 2005, 2012) |
| NGC/IC/Mrk/Arp | 1.0 | Surf. mol. CO/HCN/IR | (Gao & Solomon 2004) |
| Disc g's | $1.0 \pm 0.15$ | Surf, ALMA CO | (Leroy et al. 2013) |
| Submm g's | 0.81 - 0.84 | Surf, sub-mm | (Miettinen et al. 2017) |
| Interacting g's | $1.3 \pm 0.04$ | Surf, CO obs. | (Kaneko et al. 2022) |
| Simple average of all listed $\alpha$ | $1.056 \pm 0.192$ | (except lines 3, 4 and 5) | |

[†] Columbia 1.2 m (Dame et al. 2001), Hou et al catalogue (Hou et al. 2009), [‡] Nobeyama 45 m FUGIN and GC surveys (Umemoto et al. 2017; Tokuyama et al. 2019), WISE(Anderson et al. 2014)

10 pc, velocity dispersion $v_c \sim 5$ km s$^{-1}$, and cloud density $n_c = (100\ \text{pc})^{-3}$, we obtain a collision time of the order of $t_c \sim 20$ My. In order for the SF to proceed after the collision, it takes further $\sim 3$ to 4 My (Wu et al. 2015). These leads to a KS law with $\alpha = 2$ and $A \sim 1.0 \times 10^{-3}$. However, not only the slope but also the amplitude do not fit the observed KS law in the Milky Way (Sofue & Nakanishi 2017) even if we adjust the efficiency $\eta$ freely. So, we conclude that the cloud collision model does not apply in the Milky Way.

On the other hand, there have been a number of reports about 'evidences' for cloud-cloud collisions (Fukui et al. 2021) (and many papers cited therein). If our conclusion is correct, such evidences must be explained by other means than collision. As to the morphological evidences about the cavity of molecular-gas maps and bridge features in position-velocity diagrams, we suggest that both can be created by a molecular shell driven by an expanding HII region around the central massive stars (Sofue 2023). As to the assumption that the clouds' orbits are straight on the line of sight without angular momentum, there seems neither measurements of the transverse velocity, line-of-sight separation, nor the sense of approaching or receding, so that the orbits of the supposed colliding bodies are not determined in dynamical point of view. Also, according to the Galactic rotation, the reported mutual velocities of 5 to 30 km s$^{-1}$allow for kinematic distance of $\sim 0.1$ to 1 kpc between the two clouds. Therefore, unless these issues are clarified, there seems to be room to consider other possibilities than cloud collisions.

### 3.3 Stochastic star formation with $\alpha = 1$

We have shown that the KS-law index of the Milky Way is unity, $\alpha \simeq 1.0$, which prefers the stochastic SF scenario. A possible mechanism for stochastic SF is the self-gravitational contraction of isolated molecular clouds, which works in the scheme of the sequential star formation (Elmegreen & Lada 1977) and gravitational instability in the hubs and filaments (Myers 2009).The growth (or Jeans) time of instability in a molecular cloud of density $\sim 10^3 - 10^4$ H$_2$ cm$^{-3}$ is $t_J \sim \sqrt{1/G\rho} \sim 0.6 - 1.7$ My. If this time is regarded as the SF time, the stochastic SF is more efficient than that presumed by cloud collision time longer than a few My as above.

The global SFR is proportional to the number density $n_c$ of clouds in the averaging bins with $\delta l \times \delta v$, where the shape of the mass function of molecular clouds is assumed to be universal and the Jeans time of individual clouds with the same mass is equal to each other. On the other hand, the probability of SF in each cloud by gravitational collapse depends on the gas density and velocity dispersion inside each cloud, but not on the environment. The SFR averaged in an area sufficiently wider than clouds' size is, therefore, simply proportional to the number density of clouds, or $\alpha = 1$, which is indeed observed in the present analysis.

### 3.4 Suppression of SF in the Galactic Centre

Figure 2 showed that the SFR in the GC is comparable to that in the disc despite the much higher density of molecular gas. This indicates a significantly lower efficiency of star formation, in agreement with the current estimation of an order of magnitude lower star formation efficiency (Kruijssen et al. 2014; Barnes et al. 2017). Therefore, the SF in the GC is suppressed by some external actions such as the high magnetic pressure, fast differential rotation with strong shear, turbulence induced by explosive events in the nucleus, and/or external disturbance by falling gaseous debris from the merged companions.

### 3.5 Limitation of the analysis

We used the CO-line LVD along the Galactic plane at $b = 0^\circ$ for the molecular gas in order to represent the densest part of the disc and to avoid the complexity arising from the mixture of gases at different distances and heights. Accordingly, we constrained the HII regions to near Galactic plane objects at $|b| \lesssim 0^\circ.2$, typically $h \lesssim 20$ pc, by which about a half of the catalogued HII regions with RRL velocities was not used. This caused less number of HII regions compared to the current studies, while it avoided the uncertainty arising from the uncertain distances and heights.

Another concern is the incompleteness of the catalogued HII regions caused by the detection limit of the RRL due to decreasing fluxes with the distance. This yields apparently decreasing density of HII regions beyond several kpc (Hou & Han 2014). On the other hand the detection limit of the CO-line does not depend on the distance in so far as the molecular disc is resolved. This situation results in missing HII regions for finite CO intensity regions beyond several kpc, so that the SFR there is underestimated, and may cause a systematic error in the slope.

We checked this point by dividing the data into different longitudinal ranges, so that they represent data sets with different mean distances from the observer according to the lopsided location of the Sun in the Galaxy. As shown in table 1, we do not find significant dependence of the index on the regions. So, we consider here that the effect is rather even or negligible, not strongly disturbing the general property of KS index. However, in order to answer this question ultimately, we have to wait for an HII region catalogue sufficiently sensitive to the edge of the Galaxy.

## 4 Summary

By correlation analysis of the distributions of molecular gas and HII regions in the longitude-velocity diagrams of the Milky Way, we determined the KS index to be $\alpha \simeq 1.0$ in the Galaxy. The index is consistent with those derived in spiral galaxies for molecular gas as listed in table 1.

The unity KS index is in favor for the stochastic (spontaneous) star formation by self-regulation in individual molecular clouds, while it contradicts the cloud-collision model. We also showed that the SFR in the Galactic Centre is lower than that in the disc by an order of magnitude, indicating anomalous suppression of SF.

## Acknowledgments

The data analysis was performed at the Astronomical Data Analysis Center of the National Astronomical Observatories of Japan. The author thanks Drs. T. Umemoto (FUGIN), T. Oka (Nobeyama GC survey), T. Dame (Columbia CO survey), and L. Anderson (WISE) for making the archival data available for us.

## Data availability

The Colombia CO data were retrieved from the URL: https:// lweb.cfa.harvard.edu/ rtdc/ CO/; The WISE HII region catalogue: http:// astro.phys.wvu.edu/wise/; FUGIN Nobeyama CO survey: http://jvo.nao.ac.jp/portal; and GC CO survey: https:// www.nro.nao.ac.jp/ ~nro45mrt/html/ results/data.html

## Conflict of interest

There is no conflict of interest.

## References

Anderson, L. D., Bania, T. M., Balser, D. S., et al. 2014, ApJS, 212, 1. doi:10.1088/0067-0049/212/1/1

Bacchini, C., Fraternali, F., Iorio, G., et al. 2019, AA, 622, A64. doi:10.1051/0004-6361/201834382

Barnes, A. T., Longmore, S. N., Battersby, C., et al. 2017,

MNRAS, 469, 2263. doi:10.1093/mnras/stx941
Wu, B., Van Loo, S., Tan, J. C., et al. 2015, ApJ, 811, 56. doi:10.1088/0004-637X/811/1/56
Dame, T. M., Hartmann, D., & Thaddeus, P. 2001, ApJ, 547, 792. doi:10.1086/318388
Du, K., Shi, Y., Zhang, Z.-Y., et al. 2023, MNRAS, 518, 4024. doi:10.1093/mnras/stac3341
Elia, D., Molinari, S., Schisano, E., et al. 2022, ApJ, 941, 162. doi:10.3847/1538-4357/aca27d
Elmegreen, B. G. & Lada, C. J. 1977, ApJ, 214, 725. doi:10.1086/155302
Fuchs, B., Jahreiß, H., & Flynn, C. 2009, AJ, 137, 266. doi:10.1088/0004-6256/137/1/266
Fujita, S., Ito, A. M., Miyamoto, Y., et al. 2023, PASJ, 75, 279. doi:10.1093/pasj/psac104
Fukui, Y., Habe, A., Inoue, T., et al. 2021, PASJ, 73, S1. doi:10.1093/pasj/psaa103
Gao, Y. & Solomon, P. M. 2004, ApJ, 606, 271. doi:10.1086/382999
Habe, A. & Ohta, K. 1992, PASJ, 44, 203
Hacar, A., Clark, S. E., Heitsch, F., et al. 2023, Protostars and Planets VII, 534, 153. doi:10.48550/arXiv.2203.09562
Hasegawa, T., Sato, F., Whiteoak, J. B., et al. 1994, ApJL, 429, L77. doi:10.1086/187417
Hou, L. G., Han, J. L., & Shi, W. B. 2009, AA, 499, 473. doi:10.1051/0004-6361/200809692
Hou, L. G. & Han, J. L. 2014, AA, 569, A125. doi:10.1051/0004-6361/201424039
Kaneko, H., Kuno, N., Iono, D., et al. 2022, PASJ, 74, 343. doi:10.1093/pasj/psab129
Kennicutt, R. C. 1998, ApJ, 498, 541. doi:10.1086/305588
Kennicutt, R. C. & De Los Reyes, M. A. C. 2021, ApJ, 908, 61. doi:10.3847/1538-4357/abd3a2
Kennicutt, R. C. & Evans, N. J. 2012, ARA&A, 50, 531. doi:10.1146/annurev-astro-081811-125610
Kimura, T. & Tosa, M. 1996, AA, 308, 979
Koda, J., Scoville, N., & Heyer, M. 2016, ApJ, 823, 76. doi:10.3847/0004-637X/823/2/76
Kohno, M. & Sofue, Y. 2023, arXiv:2311.13760. doi:10.48550/arXiv.2311.13760
Komugi, S., Sofue, Y., & Egusa, F. 2006, PASJ, 58, 793. doi:10.1093/pasj/58.5.793
Komugi, S., Sofue, Y., Nakanishi, H., et al. 2005, PASJ, 57, 733. doi:10.1093/pasj/57.5.733
Komugi, S., Tateuchi, K., Motohara, K., et al. 2012, ApJ, 757, 138. doi:10.1088/0004-637X/757/2/138
Kruijssen, J. M. D., Longmore, S. N., Elmegreen, B. G., et al. 2014, MNRAS, 440, 3370. doi:10.1093/mnras/stu494
Lada, C. J. & Lada, E. A. 2003, ARA&A, 41, 57. doi:10.1146/annurev.astro.41.011802.094844
Leroy, A. K., Walter, F., Sandstrom, K., et al. 2013, AJ, 146, 19. doi:10.1088/0004-6256/146/2/19
Marasco, A., Fraternali, F., van der Hulst, J. M., et al. 2017, AA, 607, A106. doi:10.1051/0004-6361/201731054
Miettinen, O., Delvecchio, I., Smolčić, V., et al. 2017, AA, 602, L9. doi:10.1051/0004-6361/201731157
Myers, P. C. 2009, ApJ, 700, 1609. doi:10.1088/0004-637X/700/2/1609
Pineda, J. E., Arzoumanian, D., Andre, P., et al. 2023, Protostars and Planets VII, 534, 233. doi:10.48550/arXiv.2205.03935
Shu, F. H., Adams, F. C., & Lizano, S. 1987, ARA&A, 25, 23. doi:10.1146/annurev.aa.25.090187.000323
Sofue, Y. 2013, PASJ, 65, 118. doi:10.1093/pasj/65.6.118
Sofue, Y. 2017, MNRAS, 469, 1647. doi:10.1093/mnras/stx695
Sofue, Y. 2021, PASJ, 73, L19. doi:10.1093/pasj/psab078
Sofue, Y. 2023, MNRAS, 525, 4540. doi:10.1093/mnras/stad2484
Sofue, Y. 2023, Ap&SS, 368, 74. doi:10.1007/s10509-023-04231-0
Sofue, Y. & Nakanishi, H. 2016, PASJ, 68, 63. doi:10.1093/pasj/psw062
Sofue, Y. & Nakanishi, H. 2017, PASJ, 69, 19. doi:10.1093/pasj/psw123
Spilker, A., Kainulainen, J., & Orkisz, J. 2021, AA, 653, A63. doi:10.1051/0004-6361/202040021
Tokuyama, S., Oka, T., Takekawa, S., et al. 2019, PASJ, 71, S19. doi:10.1093/pasj/psy150
Umemoto, T., Minamidani, T., Kuno, N., et al. 2017, PASJ, 69, 78. doi:10.1093/pasj/psx061